

A mollified marching solution of an inverse ablation-type moving boundary problem

M. Garshasbi · H. Dastour

Received: 15 March 2014 / Revised: 16 July 2014 / Accepted: 20 August 2014 /

Published online: 4 September 2014

© SBMAC - Sociedade Brasileira de Matemática Aplicada e Computacional 2014

Abstract This study investigates the application of marching scheme and mollification method to solve a one-dimensional inverse ablation-type moving boundary problem. The problem is considered with noisy data. A regularization method based on a marching scheme and discrete mollification approach is developed to solve the proposed problem and the stability and convergence of the numerical solution are proved. Some numerical experiments are presented to demonstrate the attractiveness and feasibility of the proposed approach. It is shown that the results are in good agreement with exact solutions.

Keywords Ablation · Stefan problem · Inverse moving boundary · Marching scheme · Mollification

Mathematics Subject Classification 65M32 · 65M06 · 65M12

1 Introduction

Moving boundary problems model many real world and engineering situations in which there is freezing or melting causing a boundary to change in time (Minkowycz et al. 2009; Andrews and Atthey 1975; Carslaw and Jaeger 1959; Campbell and Humayun 1999; Ang et al. 1996). These kinds of problems describe a lot of phenomena, such as solidification of metals, freezing of water and food, crystal growth, casting, welding, melting, ablation, etc. These problems are often known as direct and inverse Stefan problems (Ang et al. 1996; Storti 1995; Mitchell and Vynnycky 2012). The direct Stefan problem requires determining both the temperature and the moving boundary interface when the initial and boundary conditions, and the thermal properties of the heat conducting body are known. Conversely, the inverse Stefan problems require determining the initial and/or boundary conditions, and/or thermal properties from additional information which may involve the partial knowledge or measurement of the

Communicated by Domingo Alberto Tarzia.

M. Garshasbi (✉) · H. Dastour

School of Mathematics, Iran University of Science and Technology, Tehran, Iran
e-mail: m_garshasbi@iust.ac.ir

moving boundary interface position, its velocity in a normal direction, or the temperature at selected interior thermocouple of the domain (Minkowycz et al. 2009; Ang et al. 1996; Mitchell and Vynnycky 2012; Molavi et al. 2011; Kwag et al. 2004; Johansson et al. 2011; Ang et al. 1996; Grzymkowski and Slota 2006).

Moreover, the inverse Stefan problems belong to a very important class of improperly posed problems of control theory which have many engineering applications. For example, in the technology of refining a material by means of recrystallization, one is interested in solving the inverse Stefan problem which consists of finding the temperature and heat flux at the fixed surface which guarantee the flatness of the crystallization front, see Minkowycz et al. (2009) and Carslaw and Jaeger (1959). We are interested in the inverse problem of parameter identification in a one-phase ablation-type moving boundary problem. The term ablation refers to the removal of material from the surface of an object by vaporization, chipping, or other erosive processes (Storti 1995; Mitchell and Vynnycky 2012; Molavi et al. 2011). The term occurs in a lot of physical situations. For example, ablative materials can sustain very high temperatures in which surface thermochemical processes are significant enough to cause surface recession. Existence of the moving boundary over a wide range of temperatures, temperature-dependent thermophysical properties of ablators, and no prior knowledge about the location of the moving surface augment the difficulty for predicting the exposed heat flux at the receding surface of ablators (Storti 1995; Mitchell and Vynnycky 2012).

In this work, an inverse ablation-type moving boundary problem is analyzed numerically using a regularization method based on the discrete mollification method and space marching scheme. The discrete mollification method is a convolution-based filtering procedure suitable for the regularization of ill-posed problems and for the stabilization of explicit schemes for the solution of partial differential equations (PDEs) (Murio 1993, 2007, 2002; Meja et al. 2001; Acosta and Meja 2008, 2009; Garshasbi et al. 2012).

The outline of this paper is as follows: In Sect. 2, the mathematical formulation of our interest inverse problem is discussed. In Sect. 3, the mollification method is introduced briefly. In Sect. 4, a numerical procedure based on marching and mollification methods is developed to solve the proposed problem. Section 5 contains the convergence and stability analysis of the introduced numerical method. In Sect. 6, some numerical examples are given and solved with the proposed method. The paper ends with conclusions in Sect. 7.

2 Description of the inverse problem

2.1 Physical interpretation

As a physical description of our interest problem, we consider a one-dimensional slab of thickness l initially at the temperature $\varphi(x)$ (Molavi et al. 2011). The surface of the slab at $x = 0$ is exposed to an unknown temperature $p(t)$, while the other surface at $x = s(t)$ is exposed to temperature and transient heat flux $q_1(t)$ and $q_2(t)$, respectively. As the slab is heated, it can chemically erode, oxidize, or change phase at the exposed surface, depending on the incident heat flux variation and the material characteristics. Hence, a moving boundary will appear in the considered domain. Generally with the presence of a source term as $f(x, t)$, the mathematical formulation for the physical problem considered here can be considered as:

$$\rho C_p(T)T_t = KT_{xx} + \rho C_p(T)H(t)T_x + f(x, t), \quad 0 < x < s(t), \quad 0 < t < T_f, \quad (1)$$

$$T(0, t) = p(t), \quad 0 < t < T_f, \quad (2)$$

$$T(s(t), t) = q_1(t), \quad 0 < t < T_f, \quad (3)$$

$$KT_x(s(t), t) = q_2(t), \quad 0 < t < T_f, \quad (4)$$

$$T(x, 0) = \varphi(x), \quad 0 \leq x \leq s(0), \quad (5)$$

where K shows the thermal conductivity and here is considered to be constant and the coefficients ρ , C_p and H show the thermophysical properties of our interest environment.

2.2 Inverse problem formulation

In the direct one-dimensional Stefan problem, we are interested to determine the moving boundary given by $x = s(t)$ and the temperature solution $u(x, t)$ in the heat conduction domain $D = (0, s(t)) \times (0, T]$, where $T > 0$ is a given arbitrary final time of interest.

In the problem (1)–(4), it is supposed that the moving boundary $s(t)$ is a known function. We are interested in the problem, which consists of determining two functions $u(x, t)$ and $p(t)$ satisfying these equations. This one-dimensional moving boundary problem can be transformed to a fixed boundary problem by a simple stretching of the spatial coordinate according $\zeta = x/s(t)$. Introducing dimensionless variables and parameters, the problem (1)–(4) is transformed into the following dimensionless form:

$$\begin{aligned} \rho C_p(u)s^2(t)u_t(\zeta, t) &= Ku_{\zeta\zeta}(\zeta, t) + \rho C_p(u)s(t) \left(\zeta \frac{ds}{dt} + H(t) \right) u_{\zeta}(\zeta, t) \\ &\quad + s^2(t)f(\zeta s(t), t), \quad 0 < \zeta < 1, \quad 0 < t < T_f, \end{aligned} \quad (6)$$

$$u(0, t) = p(t), \quad 0 < t < T_f, \quad (7)$$

$$u(1, t) = q_1(t), \quad 0 < t < T_f, \quad (8)$$

$$Ku_{\zeta}(1, t) = q_2(t), \quad 0 < t < T_f, \quad (9)$$

$$u(\zeta, 0) = \varphi(\zeta s(0)), \quad 0 < \zeta < 1. \quad (10)$$

In sequence, we will introduce a numerical marching scheme based on mollification method to find the solution of the problem (6)–(10) under the assumption that $q_1(t)$, $q_2(t)$ and $\varphi(t)$ are only known approximately as $q_1^\varepsilon(t)$, $q_2^\varepsilon(t)$ and $\varphi^\varepsilon(t)$ such that

$$\|\varphi(t) - \varphi^\varepsilon(t)\|_\infty \leq \varepsilon$$

$$\|q_1(t) - q_1^\varepsilon(t)\|_\infty \leq \varepsilon$$

$$\|q_2(t) - q_2^\varepsilon(t)\|_\infty \leq \varepsilon.$$

Because of the presence of the noise in the problem's data, we first stabilize the problem using the mollification method.

3 A brief summary of discrete mollification

Let $\delta > 0$, $\hat{p} > 0$, $A_{\hat{p}} = (\int_{-\hat{p}}^{\hat{p}} \exp(-s^2) ds)^{-1}$, $I = [0, 1]$ and $I_\delta = [\hat{p}\delta, 1 - \hat{p}\delta]$. Notice that the interval I_δ is nonempty whenever $\hat{p} < 1/2\delta$.

Furthermore, suppose $K = \{x_j : j \in \mathbb{Z}, 1 \leq j \leq M\} \subset I$, satisfying

$$x_{j+1} - x_j > d > 0, \quad j \in \mathbb{Z},$$

and

$$0 \leq x_1 < x_2 < \dots < x_M \leq 1,$$

where \mathbb{Z} is the set of integers and d is a positive constant. Now if $G = \{g_j\}_{j \in \mathbb{Z}}$ be a discrete function defined on K and $s_j = (1/2)(x_j + x_{j+1})$, $j \in \mathbb{Z}$, Then, the discrete δ -mollification of G is defined by [Murio \(1993, 2002\)](#):

$$J_\delta G(x) = \sum_{j=1}^M \left(\int_{s_{j-1}}^{s_j} \rho_\delta(x-s) ds \right) g_j,$$

where

$$\rho_{\delta, \hat{p}}(x) = \begin{cases} A_{\hat{p}} \delta^{-1} \exp\left(-\frac{x^2}{\delta^2}\right), & |x| \leq \hat{p}\delta, \\ 0, & |x| > \hat{p}\delta. \end{cases}$$

Notice that, $\sum_{j=1}^M \left(\int_{s_{j-1}}^{s_j} \rho_\delta(x-s) ds \right) = \int_{-\hat{p}\delta}^{\hat{p}\delta} \rho_\delta(s) ds = 1$.

Let $\Delta x = \sup_{j \in \mathbb{Z}} (x_{j+1} - x_j)$, some useful results of the consistency, stability, and convergence of discrete δ -mollification are as follows ([Murio 1993, 2007, 2002; Meja et al. 2001](#)):

Theorem 1 1. If $g(x)$ is uniformly Lipschitz in I and $G = \{g_j = g(x_j) : j \in \mathbb{Z}\}$ is the discrete version of g , then there exists a constant C , independent of δ , such that

$$\|J_\delta G - g\|_{\infty, I_\delta} \leq C(\delta + \Delta x).$$

Moreover, if $g'(x) \in C(I)$ then

$$\|(J_\delta G)' - g'\|_{\infty, I_\delta} \leq C \left(\delta + \frac{\Delta x}{\delta} \right).$$

2. If the discrete functions $G = \{g_j : j \in \mathbb{Z}\}$ and $G^\varepsilon = \{g_j^\varepsilon : j \in \mathbb{Z}\}$, which are defined on K , satisfy $\|G - G^\varepsilon\|_{\infty, K} \leq \varepsilon$, then we have

$$\begin{aligned} \|J_\delta G - J_\delta G^\varepsilon\|_{\infty, I_\delta} &\leq \varepsilon, \\ \|(J_\delta G)' - (J_\delta G^\varepsilon)'\|_{\infty, I_\delta} &\leq \frac{C\varepsilon}{\delta}. \end{aligned}$$

3. If $g(x)$ is uniformly Lipschitz on I , let $G = \{g_j = g(x_j) : j \in \mathbb{Z}\}$ be the discrete version of g and $G^\varepsilon = \{g_j^\varepsilon : j \in \mathbb{Z}\}$ be the perturbed discrete version of g satisfying $\|G - G^\varepsilon\|_{\infty, K} \leq \varepsilon$. Then

$$\|J_\delta G^\varepsilon - J_\delta g\|_{\infty, I_\delta} \leq C(\varepsilon + \Delta x),$$

and

$$\|J_\delta G^\varepsilon - g\|_{\infty, I_\delta} \leq C(\varepsilon + \delta + \Delta x).$$

Moreover, if $g'(x) \in C(I)$ then,

$$\begin{aligned} \|(J_\delta G^\varepsilon) - (J_\delta g)'\|_{\infty, I_\delta} &\leq \frac{C}{\delta} (\varepsilon + \Delta x), \\ \|(J_\delta G^\varepsilon)' - g'\|_{\infty, I_\delta} &\leq C \left(\delta + \frac{\varepsilon}{\delta} + \frac{\Delta x}{\delta} \right). \end{aligned}$$

Denoting the centered difference operator by \mathbf{D} , i.e., $\mathbf{D}f(x) = \frac{f(x+\Delta x)-f(x-\Delta x)}{2\Delta x}$. Then, we have the following results (Murio 1993, 2002):

Theorem 2 1. If $g' \in C^1(R^1)$ and $G = \{g_j = g(x_j) : j \in \mathbb{Z}\}$ is the discrete version of g , with G and G^ε satisfying $\|G - G^\varepsilon\|_{\infty, K} \leq \varepsilon$, then

$$\begin{aligned}\|\mathbf{D}(J_\delta G^\varepsilon) - (J_\delta g)'\|_\infty &\leq \frac{C}{\delta}(\varepsilon + \Delta x) + C_\delta(\Delta x)^2, \\ \|\mathbf{D}(J_\delta G^\varepsilon) - g'\|_\infty &\leq C \left(\delta + \frac{\varepsilon}{\delta} + \frac{\Delta x}{\delta} \right) + C_\delta(\Delta x)^2.\end{aligned}$$

2. Suppose $G = \{g_j : j \in \mathbb{Z}\}$ is a discrete function defined on a set K , and \mathbf{D}_0^δ is a differentiation operator defined by $\mathbf{D}_0^\delta(G) = \mathbf{D}(J_\delta G)(x) |_K$, then

$$\|\mathbf{D}_0^\delta(G)\|_{\infty, K} \leq \frac{C}{\delta} \|G\|_{\infty, K}.$$

4 Regularized problem and the marching scheme

The regularized problem is formulated as follows. Determine $v(x, t)$ and $p(t)$ from the following problem:

$$\begin{aligned}\rho C_p(v)s^2(t)v_t(\zeta, t) &= Kv_{\zeta\zeta}(\zeta, t) + \rho C_p(v)s(t)\{\zeta \frac{ds}{dt} + H(t)\}v_\zeta(\zeta, t) \\ &\quad + s^2(t)f(\zeta s(t), t), \quad 0 < \zeta < 1, \quad 0 < t < T_f,\end{aligned}\tag{11}$$

$$v(1, t) = J_{\delta_M}(q_1(t)), \quad 0 < t < T_f,\tag{12}$$

$$Kv_\zeta(1, t) = J_{\delta_M^*}(q_2(t)), \quad 0 < t < T_f,\tag{13}$$

$$v(\zeta, 0) = J_{\delta_i'}(\varphi(\zeta s(0))), \quad 0 < \zeta < 1,\tag{14}$$

$$v(0, t) = p(t), \quad 0 < t < T_f.\tag{15}$$

where $J_\delta(\cdot)$ shows the mollified function with respect to the mollification radii δ and the radii of mollifications, δ_0 , δ_0^* and δ' are chosen automatically using the GCV method (Murio 1993, 2007). Let M and N be positive integers, $h = \Delta x = 1/M$ and $k = \Delta t = T_f/N$ be the parameters of the finite differences discretization of $I = [0, 1]$. Let $f_1(\zeta, t) = f(\zeta s(t), t)$. We introduce the following discrete functions:

$U_{i,n}$: the discrete computed approximations of $v(ih, nk)$, $W_{i,n}$: the discrete computed approximations of $v_t(ih, nk)$, $Q_{i,n}$: the discrete computed approximations of $v_x(ih, nk)$.

The algorithm of space marching scheme may be written as follows:

1. Select δ_M , δ_M^* and δ' .
2. Perform mollification of φ^ε and q^ε in the interval $[0, 1]$.
 $U_{M,n} = J_{\delta_M} q_1^\varepsilon(nk)$ ($n \neq 0$), $U_{i,0} = J_{\delta_i'} \varphi^\varepsilon(ih s(0))$, $i \in \{0, 1, \dots, M\}$
 $Q_{M,n} = \frac{1}{K} J_{\delta_M} q_2^\varepsilon(nk)$.
3. Perform mollified differentiation in time of $J_{\delta_M} q_1^\varepsilon(nk)$. Set
 $W_{M,n} = \mathbf{D}_t(J_{\delta_M} q_1^\varepsilon(nk))$ ($n \neq 0$), $W_{M,0} = \mathbf{D}_t(J_{\delta_M'} \varphi^\varepsilon(0))$.
4. Initialize $i = M$. Do while $i \geq 1$,

$$U_{i-1,n} = U_{i,n} - h Q_{i,n}, \quad (n \neq 0),\tag{16}$$

$$\begin{aligned} Q_{i-1,n} &= Q_{i,n} - \frac{h}{K} \left[\rho C_p(U_{i,n}) \left((s(nk))^2 W_{i,n} - s(nk) \left((ih) \frac{ds}{dt}(nk) + H(nk) \right) Q_{i,n} \right) \right. \\ &\quad \left. - (s(nk))^2 f_1(ih, nk) \right], \end{aligned} \quad (17)$$

$$W_{i-1,n} = W_{i,n} - h \mathbf{D}_t \left(J_{\delta_i^*} Q_{i,n} \right) \quad (18)$$

where \mathbf{D}_t denotes the centered difference operator with respect to t . From now on, if $X_{i,n}$ is a discrete function, we denote $|X_i| = \max_n |X_{i,n}|$. We also consider $u(x, t) \in C^2(I \times I)$.

5 Stability and convergence analysis

In this section, we analyze the stability and convergence of the marching scheme (16)–(17).

Theorem 3 *For the marching scheme (16)–(17), there exists a constant Λ , such that*

$$\max\{|U_0|, |Q_0|, |W_0|, M_f\} \leq \Lambda \max\{|U_M|, |Q_M|, |W_M|, M_f\}. \quad (19)$$

Proof Let $|\delta|_{-\infty} = \min_i(\delta_i, \delta_i^*, \delta_i')$, $M_f = \max_{(\zeta, t) \in [0, 1] \times [0, 1]} \{|f_1(\zeta, t)|\}$, $M_s = \max_{t \in [0, 1]} \{s(t)\}$, $K_s = \max_{t \in [0, 1]} \{\frac{ds(t)}{dt}\}$, $M_h = \max_{t \in [0, 1]} \{H(t)\}$ and $B = \max_u \{C_p(u)\}$. Using the definition of \mathbf{D}_t and Theorem 2, one may derive

$$|\mathbf{D}_t(Q_{i,n})| \leq \frac{C}{|\delta|_{-\infty}} |Q_{i,n}|, \quad (20)$$

where C is a constant. Now using (17) and (20) we have

$$|W_{i-1,n}| \leq \left(1 + h \frac{C}{|\delta|_{-\infty}} \right) \max\{|Q_{i,n}|, |W_{i,n}|\}. \quad (21)$$

Also from (16) and (17), we have

$$|U_{i-1,n}| \leq (1 + h) \max\{|U_{i,n}|, |Q_{i,n}|\}, \quad (22)$$

$$\begin{aligned} |Q_{i-1,n}| &\leq |Q_{i,n}| + \frac{h}{K} (\rho B(M_s^2 |W_{i,n}| + M_s(K_s + M_h)|Q_{i,n}|) + M_s^2 M_f) \\ &\leq \left(1 + (\rho B M_s(M_s + K_s + M_h) + M_s^2) \frac{h}{K} \right) \max\{|Q_{i,n}|, |W_{i,n}|, M_f\}. \end{aligned} \quad (23)$$

Let $C_\delta = \max \left\{ 1, \frac{1}{K} (\rho B M_s(M_s + K_s + M_h) + M_s^2), \frac{C}{|\delta|_{-\infty}} \right\}$, from (21)–(23), we obtain

$$\max\{|U_{i-1}|, |Q_{i-1}|, |W_{i-1}|, M_f\} \leq (1 + h C_\delta) \max\{|U_i|, |Q_i|, |W_i|, M_f\},$$

and iterating this last inequality M times, we have

$$\max\{|U_0|, |Q_0|, |W_0|, M_f\} \leq (1 + h C_\delta)^M \max\{|U_M|, |Q_M|, |W_M|, M_f\}$$

which implies

$$\max\{|U_0|, |Q_0|, |W_0|, M_f\} \leq \exp(C_\delta) \max\{|U_M|, |Q_M|, |W_M|, M_f\}.$$

Letting $\Lambda = \exp(C_\delta)$ completes the proof of this statement. \square

Theorem 4 *For the marching schemes (16)–(17), for fixed δ as h, k and ε tend to zero, the discrete mollified solution converges to the mollified exact solution restricted to the grid points.*

Proof From the definitions of discrete error functions, let

$$\Delta U_{i,n} = U_{i,n} - v(ih, nk), \quad \Delta Q_{i,n} = Q_{i,n} - v_x(ih, nk), \quad \Delta W_{i,n} = W_{i,n} - v_t(ih, nk).$$

Using Taylor series, we obtain some useful equations satisfied by the mollified solution v , namely,

$$\begin{aligned} v((i-1)h, nk) &= v(ih, nk) - hv_x(ih, nk) + O(h^2), \\ v_x((i-1)h, nk) &= v_x(ih, nk) - \frac{h}{K} \left[\rho C_p(v(ih, nk)) \left((s(nk))^2 v_t(ih, nk) - s(nk) \right. \right. \\ &\quad \times \left. \left. \left((ih) \frac{ds}{dt}(nk) + H(nk) \right) v_x(ih, nk) \right) - (s(nk))^2 f_1(ih, nk) \right] + O(h^2), \\ v_t((i-1)h, nk) &= v_t(ih, nk) - h \left(\frac{d}{dt} v_x(ih, nk) \right) + O(h^2). \end{aligned}$$

On the other hand, one may write

$$\begin{aligned} \Delta U_{i-1,n} &= \Delta U_{i,n} + (U_{i-1,n} - U_{i,n}) - (v((i-1)h, nk) - v(ih, nk)) \\ &= \Delta U_{i,n} - h \Delta Q_{i,n} + O(h^2), \end{aligned} \tag{24}$$

$$\begin{aligned} \Delta Q_{i-1,n} &= \Delta Q_{i,n} + (Q_{i-1,n} - Q_{i,n}) - (v_x((i-1)h, nk) - v_x(ih, nk)) \\ &= \Delta Q_{i,n} - \frac{h}{K} \left[\rho(s(nk))^2 (w_{i,n} C_p(U_{i,n}) - v_t(ih, nk) C_p(v(ih, nk))) \right. \\ &\quad \left. - \rho(s(nk)) ((ih) \frac{ds}{dt}(nk) + H(nk)) (Q_{i,n} C_p(U_{i,n}) - v_x(ih, nk) C_p(v(ih, nk))) \right] \\ &\leq \Delta Q_{i,n} - \frac{h}{K} \left[\rho B \Delta W_{i,n} - \rho(s(nk)) ((ih) \frac{ds}{dt}(nk) + H(nk)) B \Delta Q_{i,n} \right] + O(h^2), \end{aligned} \tag{25}$$

$$\begin{aligned} \Delta W_{i-1,n} &= \Delta W_{i,n} + (W_{i-1,n} - W_{i,n}) - (v_t((i-1)h, nk) - v_t(ih, nk)) \\ &= \Delta W_{i,n} - h (\mathbf{D}_t(J_{\delta_i^*} Q_{i,n}) - v_{xt}(ih, nk)) + O(h^2). \end{aligned} \tag{26}$$

Now if in equalities (24)–(26) we use the error estimates of discrete mollification, the following inequalities are derived

$$\begin{aligned} |\Delta U_{i+1,n}| &\leq |\Delta U_{i,n}| + h |\Delta Q_{i,n}| + O(h^2), \\ |\Delta Q_{i+1,n}| &\leq |\Delta Q_{i,n}| + \frac{h}{K} (\rho B M_s (M_s |\Delta W_{i,n}| + (K_s + M_h) |\Delta Q_{i,n}|)) + O(h^2) \\ |\Delta W_{i+1,n}| &\leq |\Delta W_{i,n}| + h \left(C \frac{|\Delta Q_{i,n}| + k}{|\delta|_{-\infty}} + C_{\delta^*} k^2 \right) + O(h^2). \end{aligned}$$

Suppose

$$\begin{aligned} \Delta_i &= \max \{ |\Delta U_{i,n}|, |\Delta W_{i,n}|, |\Delta Q_{i,n}| \}, \\ C_0 &= \max \left\{ 1, \frac{1}{K} (\rho B M_s (M_s + K_s + M_h)), \frac{C}{|\delta|_{-\infty}} \right\}, \quad C_1 = \frac{ck}{|\delta|_{-\infty}} + C_{\delta^*} k^2. \end{aligned}$$

Then, we obtain

$$\Delta_{i-1} \leq (1 + hC_0)\Delta_i + hC_1 + O(h^2) \leq (1 + hC_0)(\Delta_i + C_1) + O(h^2), \tag{27}$$

and after L iterations

$$\Delta_L \leq \exp(C_0)(\Delta_M + C_1). \tag{28}$$

Moreover from

$$\begin{aligned} |\Delta U_{M,n}| &\leq C(\varepsilon + k), \\ |\Delta Q_{M,n}| &\leq C(\varepsilon + k), \\ |\Delta W_{M,n}| &\leq \frac{C}{\delta_M}(\varepsilon + k) + C_\delta k^2, \end{aligned}$$

we see that when ε, h , and k tend to 0, Δ_M and C_1 tend to 0. Consequently, $(\Delta_M + C_1)$ tends to 0 and so does Δ_0 and this completes the proof of this theorem. \square

6 Numerical results and discussion

To examine the capabilities of the proposed method, some numerical examples are considered in this section. An excellent way to check the accuracy of the numerical calculations is to compare them to the exact solutions. In all cases, without loss of generality, we set $\hat{p} = 3$ (see Murio 1993, 2007, 2002; Meja et al. 2001). The radii of mollification are always chosen automatically using the mollification and GCV methods.

Discretized measured approximations of boundary data are modeled by adding random errors to the exact data functions. For example, for the boundary data function $\phi(x, t)$, its discrete noisy version is generated by

$$\phi_{j,n}^\varepsilon = \phi(ih, nk) + \varepsilon_{j,n}, \quad i = 0, 1, \dots, N, \quad n = 0, 1, \dots, T,$$

where the $(\varepsilon_{j,n})$'s are Gaussian random variables with variance ε^2 .

The errors exact and approximate solutions are measured by the relative weighted l_2 -norm given by:

$$\frac{\left[(1/(M+1)(N+1)) \sum_{i=0}^M \sum_{j=0}^N |v(ih, jl) - U_{i,j}|^2 \right]^{1/2}}{\left[(1/(M+1)(N+1)) \sum_{i=0}^M \sum_{j=0}^N |v(ih, jl)|^2 \right]^{1/2}}.$$

All numerical results have been produced by MATLAB software.

Example 1 As the first test case, in the problem (1)–(4) consider

$$\begin{aligned} \rho &= 1, \quad C_p(T) = T, \quad K = 1, \quad H(t) = 1, \quad s(t) = \sqrt{t}, \\ f(x, t) &= 2 \sin(t^2 + x^2 + 1) - t \sin(2t^2 + 2x^2 + 2) + x \sin(2t^2 + 2x^2 + 2) \\ &\quad + 4x^2 \cos(t^2 + x^2 + 1), \\ q_1(t) &= \cos(t^2 + 1), \quad q_2(t) = 0, \\ \varphi(x) &= \cos(1). \end{aligned}$$

The exact solution may be derived as:

$$T(x, t) = \cos(t^2 + x^2 + 1), \quad (x, t) \in [0, s(t)] \times [0, 1]. \quad (29)$$

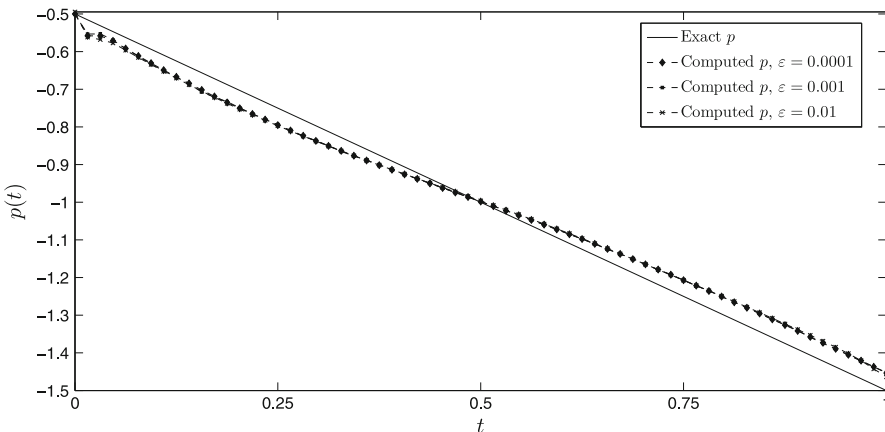
Using the exact solution for T , one may write $u(\zeta, t)$ as:

$$u(\zeta, t) = \cos(t^2 + t\zeta^2 + 1), \quad (\zeta, t) \in [0, 1] \times [0, 1].$$

Table 1 highlights the relative l_2 errors between the exact and computed u , u_t and u_x for three different noise levels $\varepsilon = 0.01, 0.001, 0.0001$ when $M = 64, 128, 256, 512$ and

Table 1 Relative l_2 error norms for Example 1

M	N	ε	u	u_t	u_ζ
64	64	0.0001	0.049877	0.056913	0.076219
128	128	0.0001	0.046497	0.05621	0.071306
256	256	0.0001	0.044996	0.053389	0.068895
512	512	0.0001	0.0446	0.052232	0.068369
64	64	0.001	0.049906	0.063412	0.076691
128	128	0.001	0.045848	0.063719	0.070531
256	256	0.001	0.045196	0.059979	0.068645
512	512	0.001	0.044518	0.053694	0.067408
64	64	0.01	0.054913	0.076445	0.076039
128	128	0.01	0.052183	0.076151	0.067892
256	256	0.01	0.05087	0.07527	0.065875
512	512	0.01	0.04901	0.073361	0.063888

**Fig. 1** The comparison between the exact and approximate $p(t)$ in three noise levels for Example 1

$N = 64, 128, 256, 512$. In this table, the l_2 errors between the exact and computed u are presented in column 4. Columns 5 and 6 include the l_2 errors between the exact and computed u_t and u_x . This table shows that increasing the amount of noise degrades the accuracy of the computed results. Furthermore, in any noise level, increasing the number of mesh points M and N decrease the amount of l_2 errors.

The comparison between the exact and the computed boundary function $p(t)$ for $M = N = 64$ and $\varepsilon = 0.01, 0.001, 0.0001$ is shown in Fig. 1. It can be found from this figure that although the measurement errors are introduced, the inverse method proposed in this work can also obtain a satisfactory solution.

To explore the dependence of errors of the solutions on the noise levels, the relative l_2 errors between the exact and computed $p(t)$ with respect to the M are shown in Fig. 2 for three noise levels when $N = 256$.

As we expected, the relative l_2 errors between the exact and numerical results were gradually decreased by increasing the mesh points.

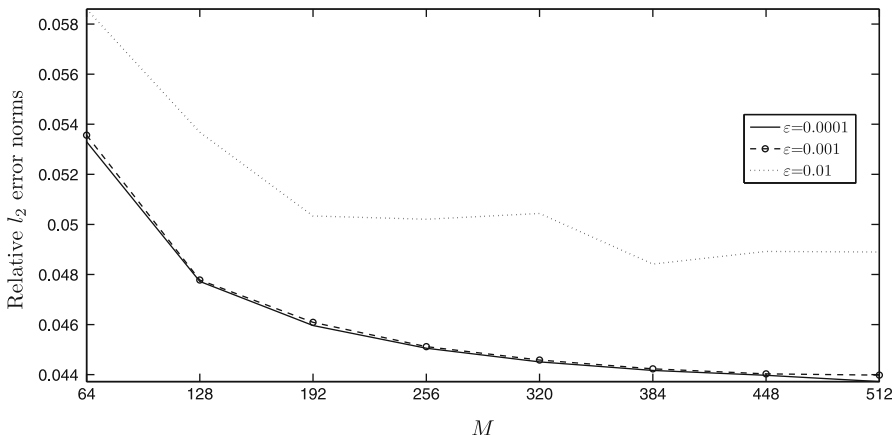


Fig. 2 The relative l_2 errors between the exact and computed $p(t)$ for three levels of noise with respect to the number of mesh points M when $N = 256$ for Example 1

Example 2 As another test case, in the problem (1)–(4) we assume

$$\begin{aligned} \rho &= 1, \quad C_p(T) = T^2, \quad K = 1, \quad H(t) = 1, \quad s(t) = \frac{1}{t+2}, \\ f(x, t) &= -2 \tanh(t + x + 1) (\tanh(t + x + 1)^2 - 1), \\ q_1(t) &= \tanh\left(t + \frac{1}{t+2} + 1\right), \quad q_2(t) = -\frac{\tanh\left(t + \frac{1}{t+2} + 1\right)^2 - 1}{t+2}, \\ \varphi(x) &= \tanh\left(\frac{x}{2} + 1\right). \end{aligned}$$

The exact solution can be obtained as:

$$T(x, t) = \tanh(t + x + 1), \quad (x, t) \in [0, s(t)] \times [0, 1]. \quad (30)$$

Using this solution, it is easy to find the exact solution for $u(\zeta, t)$ as:

$$u(\zeta, t) = \tanh\left(t + \frac{\zeta}{t+2} + 1\right), \quad (\zeta, t) \in [0, 1] \times [0, 1].$$

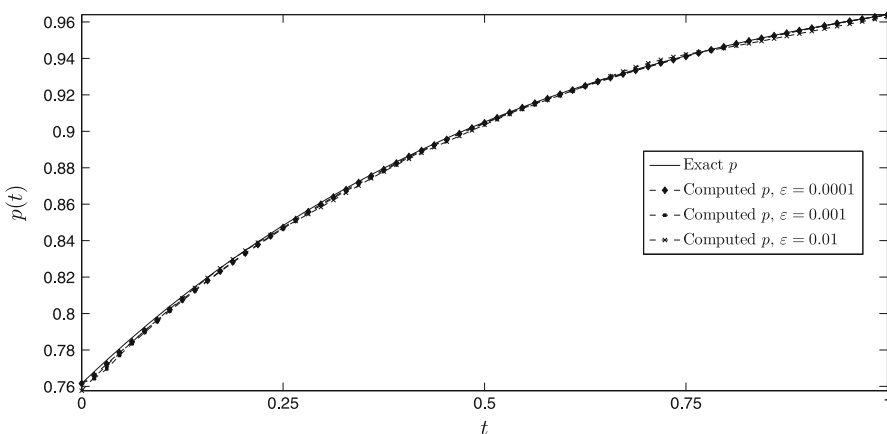
The relative l_2 errors for computing u , u_t and u_x for three different noise levels $\varepsilon = 0.01, 0.001, 0.0001$ when $M = 64, 128, 256, 512$ and $N = 64, 128, 256, 512$ are shown in Table 2. Similar to the Table 1, in this table, columns 4, 5 and 6 indicate the l_2 errors between the exact and computed u , u_t and u_x , respectively. This table shows that increasing the noise level degrades the accuracy of the computed results.

The exact and computed $p(t)$ for $M = N = 64$ and $\varepsilon = 0.01, 0.001$ and 0.0001 are shown in Fig. 3. From the three curves in this figure, one may see that when the amount of noise is considered small as $\varepsilon = 0.01, 0.001$ and 0.0001 , the numerical and analytical solutions are close to each other.

Figure 4 demonstrates the dependence of relative l_2 errors on the noise levels to compute $p(t)$. In this figure for three different noise levels $\varepsilon = 0.01, 0.001$ and 0.0001 , the relative l_2 error is plotted with respect to the number of mesh points M when $N = 256$. In this example, we see that increasing the number of mesh points has not a considerable effect on the amount

Table 2 Relative l_2 error norms for Example 2

M	N	ε	v	v_t	v_ζ
64	64	0.0001	0.00033448	0.013541	0.021461
128	128	0.0001	0.00049445	0.013932	0.023045
256	256	0.0001	0.00057725	0.018173	0.024004
512	512	0.0001	0.00061985	0.021169	0.024973
64	64	0.001	0.00058512	0.02624	0.023947
128	128	0.001	0.00081867	0.032996	0.027673
256	256	0.001	0.00098191	0.050765	0.033719
512	512	0.001	0.0010456	0.061915	0.03563
64	64	0.01	0.0013711	0.12292	0.042667
128	128	0.01	0.0010493	0.065805	0.038562
256	256	0.01	0.0011946	0.051633	0.026394
512	512	0.01	0.0011558	0.16973	0.046342

**Fig. 3** The comparison between the exact and approximate $p(t)$ in three noise levels for Example 2

of relative l_2 error. Whereas decreasing the amount of noise increases the accuracy of the numerical results.

7 Conclusions

In this study, an explicit and unconditionally stable space marching finite difference method has been implemented to solve a one-dimensional nonlinear inverse Stefan problem. Overall, from the numerical results presented in this paper and in some previous studies (see Acosta and Meja 2008, 2009), it can be concluded that the combination of discrete mollification and explicit space-marching finite difference methods is a suitable technique for the identification of some unknown boundary functions in initial boundary value problems. Discrete mollification is a stabilizer and accelerator for explicit numerical schemes which can be used to solve many class of PDEs, such as hyperbolic conservation laws and parabolic equations (Meja et al. 2001; Acosta and Meja 2008, 2009). The algorithm effectively restores stability

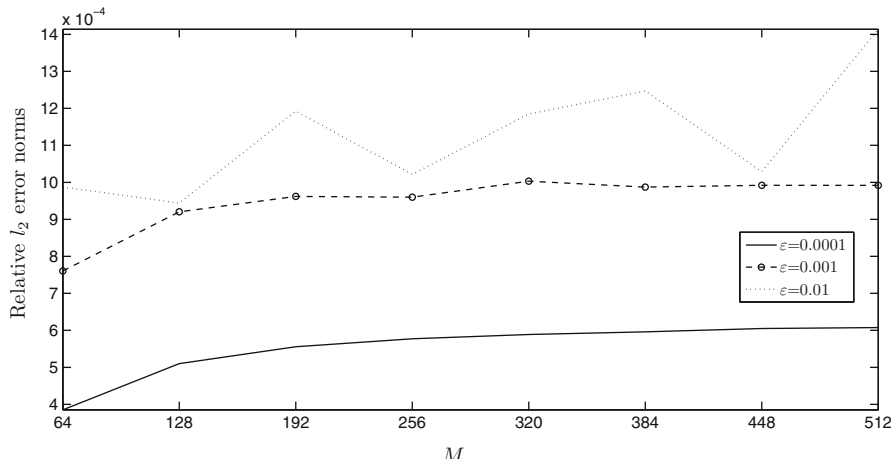


Fig. 4 The relative l_2 errors between the exact and computed $p(t)$ for three levels of noise with respect to the number of mesh points M when $N = 256$ for Example 2

with respect to perturbations in the data, which is essential to justify the introduction of the inverse problem approaches. In comparison with some other approaches such as classical finite difference schemes and finite element methods, the numerical procedure proposed in this paper is easy to implement and avoids, for example, the necessity of solving systems of nonlinear equations or least square problems. Changing the noise level did not seem to change the shape of the approximation, except for t close to the final time T . It should be pointed out that in the presence of noise, the ideal expected behavior of parameters and errors is: when h , k and δ tend to zero, the error tends to zero too. However, many factors intervene and this is not always the case (see Table 2). Only some values of h are appropriate to reduce the error. It is important to recall that we are dealing with random noise and with automatic procedures such as GCV for the selection of mollification parameters. Sometimes, these procedures do not select optimal values. Fortunately, this happens only occasionally, as can be seen from the reliability tests presented above. In addition, the numerical algorithm presented in this study is only first-order accurate, so moderate errors should be expected.

Acknowledgments The authors would like to thank the anonymous referees for their valuable comments and suggestions which substantially improved the manuscript.

References

- Acosta CD, Meja CE (2008) Stabilization of explicit methods for convection diffusion equations by discrete mollification. *Comput Math Appl* 55:368–380
- Acosta CD, Meja CE (2009) Approximate solution of hyperbolic conservation laws by discrete mollification. *Appl Numer Math* 59:2256–2265
- Andrews G, Atthey DR (1975) On the motion of an intensely heated evaporating boundary. *J Inst Math Appl* 15:59–72
- Ang DD, Dinh APN, Tranh D (1996) An inverse Stefan problem: identification of boundary value. *J Comput Appl Math* 66:75–84
- Ang DD, Dinh APN, Tranh D (1996) An inverse Stefan problem. *J Comput Appl Math* 66:75–84
- Campbell AJ, Humayun M (1999) Trace element microanalysis in iron meteorites by laser ablation, ICPMS. *Anal Chem* 71(5):939–946

- Carslaw HS, Jaeger JC (1959) Conduction of heat in solids, 2nd edn. Clarendon Press, Oxford
- Garshasbi M, Reihani P, Dastour H (2012) A stable numerical solution of a class of semi-linear Cauchy problems. *J Adv Res Dyn Cont Syst* 4:56–67
- Grzymkowski R, Slota D (2006) One-phase inverse Stefan problem solved by Adomain decomposition method. *Comput Math Appl* 51:33–40
- Johansson BT, Lesnic D, Reeve T (2011) A method of fundamental solutions for the one-dimensional inverse Stefan problem. *Appl Math Model* 35:4367–4378
- Kwag DS, Park IS, Kim WS (2004) Inverse geometry of estimating the phase front motion of ice in a thermal storage system. *Inv Prob Sci Eng* 12:743–756
- Meja CE, Murio DA, Zhan S (2001) Some applications of the mollification method. In: Lassonde M (ed) *Appl. optim. math. econ.* Physica-Verlag, pp 213–222
- Minkowycz WJ, Sparrow EM, Murthy JY (2009) Handbook of numerical heat transfer, 2nd edn. Wiley, New York
- Mitchell SL, Vynnycky M (2012) An accurate finite-difference method for ablation-type Stefan problems. *J Comput Appl Math* 236:4181–4192
- Molavi H, Hakkaki-Fard A, Molavi M, Rahmani RK, Ayasoufi A, Noori S (2011) Estimation of boundary conditions in the presence of unknown moving boundary caused by ablation. *Int J Heat Mass Trans* 54:1030–1038
- Murio DA (2002) Mollification and space marching. In: Woodbury K (ed) *Inverse engineering handbook*. CRC Press, USA
- Murio DA (1993) The mollification method and the numerical solution of ill-posed problems. Wiley-Interscience, New York
- Murio DA (2007) Stable numerical solution of a fractional-diffusion inverse heat conduction problem. *Comput Math Appl* 53:1492–1501
- Storti M (1995) Numerical modeling of ablation phenomena as two-phase Stefan problems. *Int J Heat Mass Trans* 38:2843–2854